Synthetic Metals 209 (2015) 484–489

Contents lists available at ScienceDirect

Synthetic Metals

journal homepage: www.elsevier.com/locate/synmet

Efficient quantum dot light emitting devices with ethanol treated PEDOT: PSS hole injection layer

Jia Wang[a,b], Han Zhang[b], Wenyu Ji[a,*], Hanzhuang Zhang[b,*]

[a] State Key Laboratory of Luminescence and Applications, Changchun Institute of Optics, Fine Mechanics and Physics, Chinese Academy of Sciences, Changchun 130033, China
[b] Department of Physics, Jilin University, Changchun 130023, China

ARTICLE INFO

Article history:
Received 6 June 2015
Received in revised form 25 August 2015
Accepted 31 August 2015
Available online 12 September 2015

Keywords:
Quantum dots
Light emitting diodes
Hole-injection layer
PEDOT:PSS

ABSTRACT

The conductivity of poly(3,4-ethylenedioxythiophene)-poly(styrene sulfonate) (PEDOT:PSS) film is improved by simply mixing PEDOT:PSS solution with ethanol for the film deposition, and the performance of quantum-dot light-emitting diodes (QD-LEDs) is significantly enhanced with ethanol treated (ET- treated) PEDOT:PSS as the hole injection layer (HIL). Comparing with the pristine PEDOT:PSS based device, the current density of device with ET-treated PEDOT:PSS as the HIL is increased by 18%, from 50 to 59 mA/cm^2, at operating voltage of 5 V, and the maximum current efficiency is enhanced by 12.5%, from 10.4 to 11.7 cd/A, which is due to the improved conductivity of ET-treated PEDOT:PSS film. With atomic force microscopy (AFM) measurements, we demonstrate that the improvement of the conductivity of PEDOT:PSS film is due to the decreased PSSH amount after solvent treatment, reducing the thickness of PSSH insulating shell, leading to an efficient charge transport across the PEDOT chains.

1. Introduction

Due to unique optoelectronic properties and high emission quantum yield, which are strongly dependent on their size, semiconductor II–VI quantum dots have been paid extensively attention to the potential applications in flat panel displays and solid-state lighting sources [1–6]. Especially, quantum dot light-emitting devices (QD-LEDs) with near 100% internal quantum efficiency was reported by Shirasaki et al. [6], offering significant advantages over organic LEDs [7,8]. Many efforts were devoted to the QD-LED field to improve the device performance, closing to that of organic LEDs [9,10]. To date, the most efficient device is achieved through a hybrid structure, consisting of organic carrier transport layers combined with an inorganic metal oxide electron transport layer (ETL), such as poly(3,4-ethylenedioxythiophene)-poly(styrene sulfonate) (PEDOT:PSS) hole injection layer (HIL), CBP hole transport layer (HTL), poly[-*bis*(4-butylphenyl)–*bis*(phenyl) benzidine] (poly-TPD) HTL, ZnO nanoparticle ETL, and TiO_2 electron transport layer [9–16]. Recently, an efficient QD-LEDs with an external quantum efficiency (EQE) of 20.5% was reported by employing ZnO nanoparticle as the ETL combined with organic HTLs [10], benefitting from the outstanding properties of ZnO ETL, including high electron mobility, matched energy level with QDs and good stability. Meanwhile, the QDs/ZnO interface was modified by a thin poly(methylmethacrylate) layer to suppress the exciton quenching induced by the ZnO, which plays an important role in improving the device efficiency. So far the ZnO nanoparticle film is demonstrated the best candidate as the ETL and highly efficient QD-LEDs have been fabricated [10–18]. Enlightened from the effect of efficient electron injection and interface engineering achieved by the ZnO ETL on the device performance [10], optimizing HTL/HIL to achieve efficient hole injection must be a feasible strategy to improve the QD-LED performance.

In common QD-LEDs, the PEDOT:PSS is often used as the HIL to enhance the ITO work function and hole injection from ITO to HTL. It has been widely accepted that high resistivity of the PEDOT:PSS film could lead to a higher average electric field across the device, and more Joule heating, which would substantially deteriorate the device performance [19]. Therefore, increasing the conductivity of PEDOT:PSS is beneficial to improve device performance. It is well known that the conjugated polymer PEDOT is positively doped, and the sulfonate anionic groups of PSS are used as the counterions to balance the doping charges. PEDOT:PSS films after secondary doping with some inert solvents, such as sorbitol [20,21], *N*-methylpyrrolidone [22], (poly)-ethylene glycol and other alcohols [19,23,24], dimethyl sulfoxide (DMSO), *N*,*N*-dimethylformamide, and tetrahydrofuran [25], lead to a conductivity increase

* Corresponding author.
E-mail addresses: jiwy@ciomp.ac.cn, jlu__jwy@163.com (W. Ji), zhanghz@jlu.edu.cn (H. Zhang).

http://dx.doi.org/10.1016/j.synthmet.2015.08.033
0379-6779/

of 2-3 orders of magnitudes to reach up to 80 S/cm. A methanol treated high conductivity PEDOT:PSS film has been used in the organic LEDs [26], which results in an improvement in the device performance, including lower operating voltage, higher luminance and efficiency. However, there are not any reports on optimizing the PEDOT:PSS film to improve QD-LED perfromance.

In this work, we demonstrate that the performance of QD-LEDs with ethanol-treated (ET-treated) PEDOT:PSS as the HIL is improved dramatically. The device luminance, current density, and efficiency are all higher than that of pristine PEDOT:PSS based device, which is attributed to the improvement of conductivity of ET-treated PEDOT:PSS film due to the formation of continuous conducting PEDOT:PSS domains and reduced PSS component.

2. Experiments and characterizations

QD-LEDs with a structure of ITO/PEDOT:PSS (30 nm)/poly-TPD (40 nm)/QDs (25 nm)/ZnO (45 nm)/Al (100 nm) were built. The PEDOT:PSS, poly-TPD, QDs, ZnO, and Al were used as HIL, HTL, emission layer, ETL, and cathode, respectively. Before use, all the ITO substrates with a square resistance of 12 Ω/square were ultrasonically cleaned in acetone, ethanol, deionized water, and isopropanol in sequence and followed by an *ex situ* UV ozone treatment in air for 5 min. PEDOT:PSS (Clevios™ P Al 4083) was spin-cast at 3000 rpm for 60 s to form a film of 30 nm thickness. In order to investigate the effect of ethanol on the device performance, the PEDOT:PSS diluted with ethanol (the volume rate of PEDOT:PSS to ethanol is 1:1) and deionized water (the rate of PEDOT:PSS to water is 8:1) were used for device A and B, respectively. The PEDOT:PSS films were annealed at 120 °C for 30 min in air to obtain a highly conductive layer. Subsequently, the HTL of poly-TPD was spin-coated onto the HIL at 2500 rpm from a 0.8 wt% chlorobenzene solution and dried at 100 °C in a glove box (MBRAUN) for 30 min to give a high quality, homogeneous layer of approximately 40 nm. Then, the QD layer was deposited onto the poly-TPD by spin-coating at a speed of 2000 rpm from toluene solutions of QDs (12 mg/ml) and then annealed at 70 °C for 30 min in the same glove box. The thickness of QD layer was ~25 nm estimated from cross-section scanning electron microscopic (SEM) image. The ZnO nanoparticles were then deposited onto the QDs by spin-coating process at a speed of 2000 rpm from a 30 mg/ml ZnO ethanol solution and then annealed at 120 °C for 30 min in the same glove box. The thickness of ZnO layer is around 45 nm. Finally, the cathode of Al (100 nm) was thermally evaporated in high vacuum at pressure below 4×10^{-6} Torr. The Al cathode lines with a width of 2.5 mm were deposited orthogonally to the ITO anode lines to form a 5 mm^2 pixel. The ZnO nanoparticles and red CdSe/ZnS core–shell QDs were synthesized with a method proposed in previous reports [12,27].

Detailed measurement processes for QD-LEDs have been described in our previous report [11]. The spectra of the devices were measured with an Ocean Optics Maya 2000-PRO spectrometer. The room temperature absorption spectrum was measured with an ultraviolet/visible spectrometer (UV 1700, Shimadzu) and the PL spectrum was collected by a Hitachi F-4500 spectrophotometer under an excitation wavelength of 400 nm. Note that the absorption and PL spectra were obtained from the QD toluene solution. The transmission electron microscopy (TEM) images were recorded on a Philips TECNAI G2 and SEM images were measured with by a Hitachi S4800. Atomic Force Microscopy (AFM) images were recorded in the tapping mode by Bruker Multimode-8.

3. Results and discussion

Fig. 1a shows the absorption and photoluminescence (PL) spectra of CdSe/ZnS QDs in toluene. The emission peak is 600 nm with a full-width at half maximum of 42 nm. The PL spectrum exhibits a good Gaussian profile and not any defect emission is observed, which indicate an efficient exciton recombination and confinement in CdSe core. It is worth noting that the characteristic exciton absorption peaks are not distinct in these QDs, which should be attributed to the formation of alloy transition layer at CdSe core and ZnS shell interface in the QD. The uniformity and monodispersion of QDs synthesized in this work is characterized by TEM measurements and the results are shown in Fig. 1b. We can see that the QDs exhibit high monodispersion and the diameter of QDs is around 9 nm. The inset of Fig. 2b shows a high resolution TEM image of single QD. Noting that not any distinct boundary between the core and shell is observed, which is attributed to the continuous composition gradient and alloy transition interface inside the QDs, in accordance with the absorption data exhibited in Fig. 1a. Fig. 1c shows a photo of a vial of CdSe/ZnS QD solution exited under 365 nm light, exhibiting a vivid red emission from the QDs. The quantum yield of CdSe/ZnS QDs is 50% in solid powder form measured through an integrating sphere. QD-LEDs based on red CdSe/ZnS were fabricated with the typical device structure via all solution processes for the constituent layers as shown in Fig. 2a. The QD emission layer is sandwiched between poly-TPD HTL and ZnO nanoparticle ETL. The Al cathode is deposited by thermal evaporation technique and all the devices are measured without any encapsulation. The flat energy levels of the materials used in our study are shown in Fig. 2b. The highest occupied molecule orbital (HOMO) and the lowest unoccupied molecule orbital (LUMO) energy levels are cited from the literatures [28,29]. Based on the energy level alignment between QDs and poly-TPD, it can be inferred that the excitons must be formed at QD/poly-TPD interface due to the large barriers to electrons (~2.0 eV) and holes (~1.0 eV). Therefore, the QD/poly-TPD interface becomes very crucial to the device performance. Moreover, it is well known that the quality of

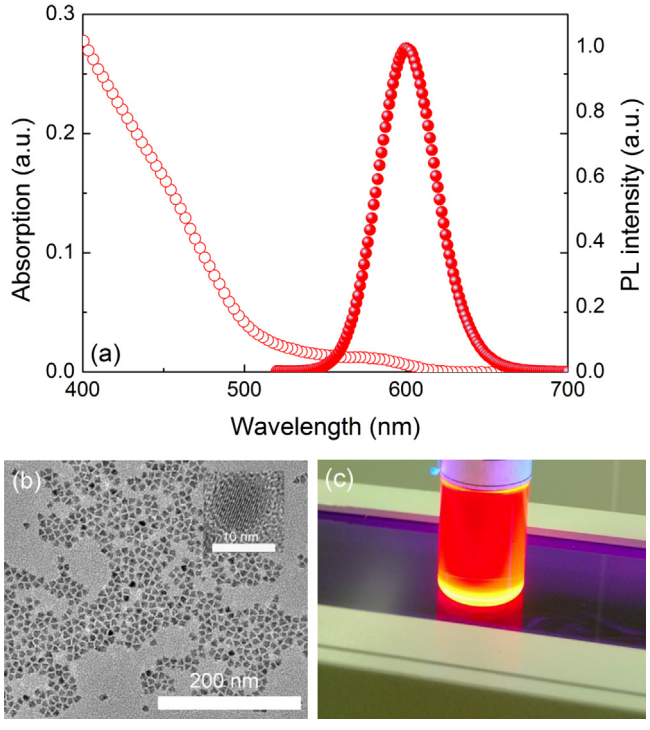

Fig. 1. (a) Absorption and PL spectra of QDs in toluene; (b) TEM image of the CdSe/ZnS core/shell QDs; (c) the representative UV-illuminated photo of QDs dispersion in toluene.

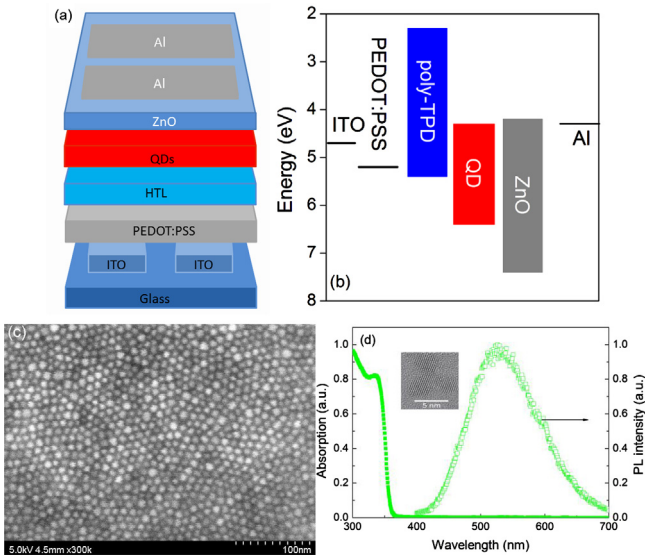

Fig. 2. (a) The structure schematic diagram of the QD-LEDs in our work; (b) energy level diagram for the various layers; (c) SEM images of CdSe/ZnS QDs on ITO/poly-TPD/ PEDOT:PSS; (d) absorption and PL spectra of ZnO nanoparticles in ethanol. Inset is TEM image of ZnO nanoparticles.

QD film plays a key role in QD-LED performance. The morphology of QD film on the ZnO layer is characterized by the SEM image shown in Fig. 2c. We can see that a homogeneous and close-packed QD layer is obtained, which ensures the successive fabrication and reproduction of efficient QD-LEDs. The thicknesses of QD is ~25 nm obtained through the cross-section SEM images of ITO/ZnO and ITO/ZnO/QDs samples, and data are not shown here. The ZnO nanoparticles were synthesized according to the method reported previously, [12] with a diameter of 3–5 nm and PL peak at 530 nm as shown in Fig. 2d. The exciton absorption peak is about 335 nm, according to an estimated bandgap of 3.7 eV.

As we know, the thickness of each layer dramatically influences the electrical properties of QD-LEDs. In all the devices, the QD and ZnO layers were deposited under the same conditions. Therefore, their thicknesses will be identical with each other within the experimental error range. In order to eliminate the effect of thickness variation of PEDOT:PSS and poly-TPD films on the device electrical properties, we carefully adjust the concentration of PEDOT:PSS with and without ethanol to achieve identical layer thicknesses. The thicknesses are measured for single layer PEDOT:PSS and bilayer PEDOT:PSS/poly-TPD films fabricated under the same conditions to that of device A and B as described in Section 2, which is 30 nm for PEDOT:PSS layers (with and without ethanol treating) and 70 nm for PEDOT:PSS/poly-TPD films. In other words, the thicknesses of HILs and HTLs in device A and B are the same, which ensures a fair comparison for the device performance between device A and B. The current density–voltage–luminance curves of QD-LEDs are shown in Fig. 3a. As can be seen, the current density of ET-treated device is increased by 18%, from 50 to 59 mA/cm^2 at operating voltage of 5 V, compared with that pristine PEDOT:PSS based device. Considering the discussed above, the enhancement for the current density must originate from the ET-treated PEDOT:PSS layer and the mechanism will be exploited later in detail. In addition, we can see that the device luminance is also enhanced dramatically for the ET-treated device compared to that of a device based on pristine PEDOT:PSS in whole operation voltage range. For example, the luminance is 3326, and 2675 cd/m^2 for devices A and B, respectively, at the operation voltage of 4.5 V. And an enhancement factor of 24% is obtained. However, the maximum luminance of these two devices is 40,520 and 39,050 cd/m^2 respectively, achieved at 7.5 V. It is very strange that the corresponding enhancement factor is decreased to only 4%. The decreased enhancement factor with increased current density reveals that the charge carriers injected into the QDs should be saturated under high applied current densities. Therefore, the effect of charge carrier mobility of PEDOT:PSS becomes rather weak and exciton quenching processes dominates the device performance. As a result, these two devices exhibit similar performance due to the same electroluminescence mechanism and environment (exciton formation interface) for excitons in both devices A and B under high operation voltages. As reported previously, the current density of 100 mA/cm^2 is high enough to excite all the QDs at the exciton formation interface considering the exciton lifetime (on the order of tens of nanoseconds) [30]. In other words, the most efficiently radiative decay for the excitons should be achieved at low current density in order to prevent nonradiative decay processes, such as Auger recombination and QD charging quenching processes. This hypothesis is confirmed by the efficiency-current density characteristics shown in Fig. 3b that the maximum efficiency is obtained at low current density near 20 mA/cm^2. However, the current efficiency of the ET-treated PEDOT:PSS based QD-LED is higher than that of device with pristine PEDOT:PSS as the HIL at whole applied current density

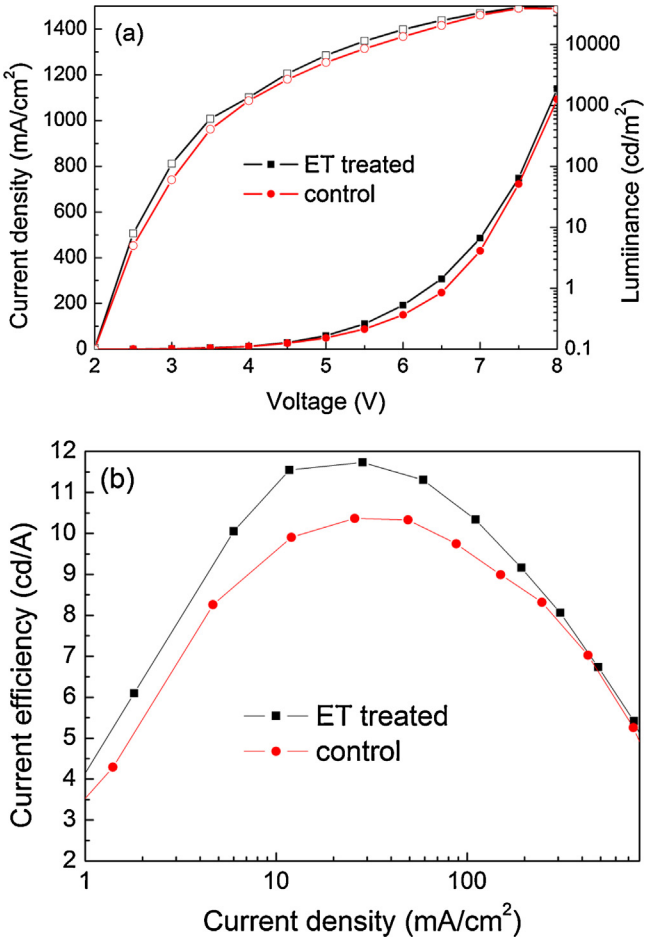

Fig. 3. (a) The current density–voltage–luminance and (b) efficiency–current density curves of QD-LEDs.

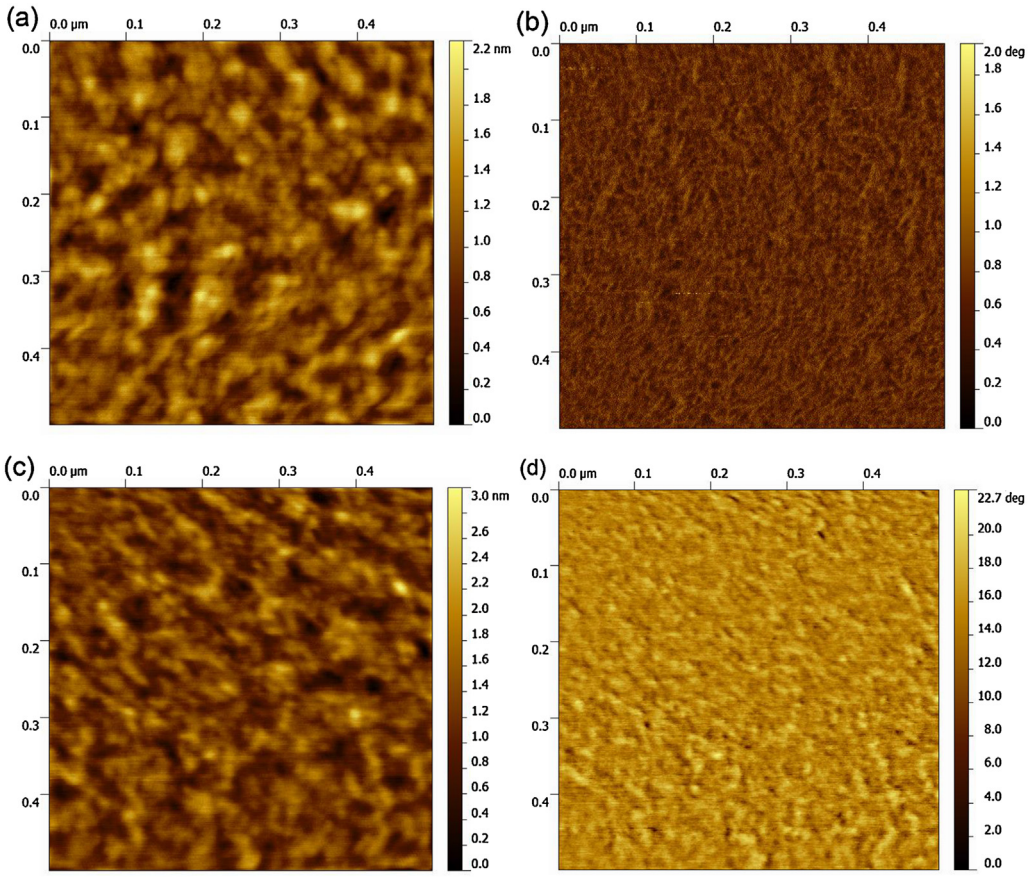

Fig. 4. Topography (a and c) and phase images (b and d) of the without solvent treated (a and b) and with ET-treated (c and d) for the PEDOT:PSS films on ITO substrates.

range, indicating the important role of ET-treating process in improving the device performance. For the ET-treated PEDOT:PSS based device, the maximum efficiency is increased from 10.4 cd/A to 11.7 cd/A and an enhancement factor of 12.5% is achieved.

In order to investigate the effect of ethanol on the properties of PEDOT:PSS film, we carefully implement AFM measurement with a tipping-mode. Fig. 4a and c shows the topography of 0.5 μm × 0.5 μm of PEDOT:PSS film without and with ET-treating. Grains are observed on the surface of both films. But more elongated structures are observed for ET-treated film as can be seen from Fig. 4c. Consequently, the pristine PEDOT:PSS film has a surface roughness of 0.28 nm and after treating with ethanol, the surface roughness increases to 0.34 nm. The rougher surface caused by ethanol treatment should originate from the swelling and softening of the PEDOT:PSS film by the ethanol solvent as reported by Wang et al. [26]. In addition, the added ethanol thus induces a phase separation on the nanometer scale characterized by a segregation of the excess PSS in domains surrounded by a PEDOT-PSS phase. The corresponding phase images of PEDOT:PSS films without and with ethanol treating confirm this hypothesis as shown in Fig. 4b and d. It has been demonstrated that, for polymer systems, a lower phase angle means a softer material, whereas a higher phase angle can be identified with a harder material. This means that the bright regions in Fig. 4b and d could be attributed to the PEDOT-PSS domains, while the dark regions appeared dark ascribed to the excess PSS domains. After treating with ethanol solvent, the phase image shows a phase separation characterized by segregation of the excess PSS domains surrounded by a continuous PEDOT:PSS phase, i.e. the dark area, is greatly reduced, which is consistent with the results reported by Wang et al. [26]. It has been revealed that the neat PEDOT:PSS solid film exhibits the core-shell structure, in which the core is rich in conducting PEDOT surrounded by the insulating PSS [31]. The continuous conducting PEDOT:PSS domains and reduced PSS component ultimately improve the conductivity of PEDOT:PSS film. Therefore, the conductivity enhancement of PEDOT:PSS is responsible to the improvement of device performance and stability.

Fig. 5a shows the electroluminescence (EL) spectra of the devices at a driving voltage of 5 V. As can be seen, a pure and saturated red emission completely originating from QDs is observed for all the QD-LEDs, and not any emission at the low-energy region in the EL spectra is occurred. The full-width at half maximum of EL spectrum is 46 nm, similar to that of PL spectrum (42 nm). All the results indicate a highly radiative recombination efficiency originating from QD band emission. The emission stability of QD-LED with ET-treated PEDOT:PSS as the HIL is demonstrated by characterizing the EL emission profile at different operating voltages as shown in Fig. 5b. As can be seen, the EL emission is very stable with almost the same emission peak and profile at different operating voltage range from 4 to 7 V. The EL spectra of QD-LED with pristine PEDOT:PSS HIL were also measured at different voltages and the same trend was observed. These results indicate that the exciton recombination zone in QD-LEDs should not be changed at different electric field applied to the devices.

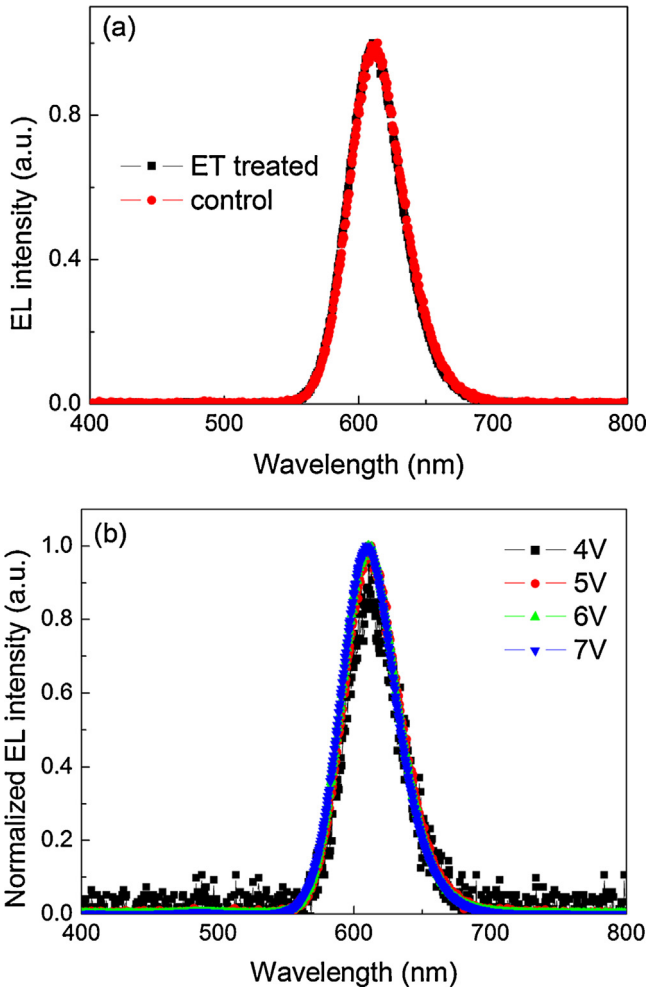

Fig. 5. (a) EL spectra of QD-LEDs with and without ET-treated PEDOT:PSS HIL at voltage of 4.5 V; (b) EL spectra of QD-LEDs based on ET-treated PEDOT:PSS HIL at different voltages.

4. Conclusion

The conductivity of PEDOT:PSS film was enhanced through simple ET-treating process, directly mixing PEDOT:PSS solution with ethanol solvent. The added ethanol induces a phase separation on the nanometer scale characterized by a segregation of the excess PSS in domains surrounded by a PEDOT-PSS phase, which leads to an efficient charge transport across the PEDOT chains. The device performance of QD-LEDs was improved by introducing an ET-treated PEDOT:PSS as the HIL. The overall performance of device containing ET-treated PEDOT:PSS was improved compared with the pristine PEDOT:PSS based device, the current efficiency was increased by a factor of 12.5%, from 10.4 cd/A to 11.7 cd/A. The solvent treatment process for the HIL is simple, efficient, cost-effective and easy to be adopted in mass production. We believe that our work provides a feasible and reliable approach to construct efficient QD-LEDs for both display and solid-state lighting technologies.

Acknowledgment

This work was supported by the National Natural Science Foundation of China (Nos. 61205025, 11204298, 11474131, and 11274142).

References

[1] V.L. Colvin, M.C. Schlamp, A.P. Alivisatos, Light-emitting-diodes made from cadmium selenide nanocrystals and a semiconducting polymer, Nature 370 (1994) 354–357.
[2] B.K. Chen, H.Z. Zhong, W.Q. Zhang, Z.A. Tan, Y.F. Li, C.R. Yu, T.Y. Zhai, Y.S. Bando, S.Y. Yang, B.S. Zou, Highly emissive and color-tunable CuIns2-based colloidal semiconductor nanocrystals: off-stoichiometry effects and improved electroluminescence performance, Adv. Funct. Mater. 22 (2012) 2081–2088.
[3] Y. Zhang, C. Xie, H.P. Su, J. Liu, S. Pickering, Y.Q. Wang, W.W. Yu, J.K. Wang, Y.D. Wang, J.I. Hahm, N. Dellas, S.E. Mohney, J. Xu, Employing heavy metal-free colloidal quantum dots in solution-processed white light-emitting diodes, Nano Lett. 11 (2011) 329–332.
[4] H.B. Shen, X.W. Bai, A. Wang, H.Z. Wang, L. Qian, Y.X. Yang, A. Titov, J. Hyvonen, Y. Zheng, L.S. Li, High-efficient deep-blue light-emitting diodes by using high quality ZnxCd1-xS/ZnS core/shell quantum dots, Adv. Funct. Mater. 24 (2014) 2367–2373.
[5] V. Wood, V. Bulović, Colloidal quantum dot light-emitting devices, Nano Rev. 1 (2010) 5202.
[6] Y. Shirasaki, G.J. Supran, M.G. Bawendi, V. Bulović, Emergence of colloidal quantum-dot light-emitting technologies, Nat. Photonics 7 (2013) 13–23.
[7] E. Matioli, S. Brinkley, K. Kelchner, Y. Hu, S. Nakamura, S. DenBaars, J. Speck, C. Weisbuch, High-brightness polarized light-emitting diodes, Light Sci. Appl. 1 (2012) e22.
[8] C. Xiang, W. Koo, F. So, H. Sasabe, J. Kido, A systematic study on efficiency enhancements in phosphorescent green, red and blue microcavity organic light emitting devices, Light Sci. Appl. 2 (2013) e74.
[9] Y.X. Yang, Y. Zheng, W.R. Cao, A. Titov, J. Hyvonen, J.R. Manders, J.G. Xue, P.H. Holloway, L. Qian, High-efficiency light-emitting devices based on quantum dots with tailored nanostructures, Nat. Photonics 9 (2015) 259–266.
[10] X.L. Dai, Z.X. Zhang, Y.Z. Jin, Y. Niu, H.J. Cao, X.Y. Liang, L.W. Chen, J.P. Wang, X.G. Peng, Solution-processed, high-performance light-emitting diodes based on quantum dots, Nature 515 (2014) 96–100.
[11] W.Y. Ji, P.T. Jing, J.L. Zhao, X. Liu, A. Wang, H. Li, Inverted CdSe/CdS/ZnS quantum dot light emitting devices with titanium dioxide as an electron-injection contact, Nanoscale 5 (2013) 470–476.
[12] J.H. Kwak, W.K. Bae, D.G. Lee, I. Park, J.H. Lim, M.J. Park, H.D. Cho, H.J. Woo, D.Y. Yoon, K.H. Char, S.H. Lee, C.H. Lee, Bright and efficient full-color colloidal quantum dot light-emitting diodes using an inverted device structure, Nano Lett. 12 (2012) 2362–2366.
[13] B.S. Mashford, M. Stevenson, Z. Popovic, C. Hamilton, Z. Zhou, C. Breen, J. Steckel, V. Bulovic', M. Bawendi, S. Coe-Sullivan, P.T. Kazlas, High-efficiency quantum-dot light-emitting devices with enhanced charge injection, Nat. Photonics 7 (2013) 407–412.
[14] W.K. Bae, Y.-S. Park, J. Lim, D. Lee, L.A. Padilha, H. McDaniel, I. Robel, C. Lee, J.M. Pietryga, V.I. Klimov, Controlling the influence of Auger recombination on the performance of quantum-dot light-emitting diodes, Nat. Commun. 4 (2013) 2661.
[15] H.B. Shen, W.R. Cao, N.T. Shewmon, C. Yang, L.S. Li, J.G. Xue, High-efficiency, low turn-on voltage blue–violet quantum-dot-based light-emitting diodes, Nano Lett. 15 (2015) 1211–1216.
[16] H.H. Kim, S. Park, Y. Yi, D.I. Son, C. Park, D.K. Hwang, W.K. Choi, Inverted quantum dot light emitting diodes using polyethylenimine ethoxylated modified ZnO, Sci. Rep. 5 (2015) 8968.
[17] J. Lim, B.G. Jeong, M. Park, J.K. Kim, J.M. Pietryga, Y.S. Park, V.I. Klimov, C.H. Lee, D.C. Lee, W.K. Bae, Influence of shell thickness on the performance of light-emitting devices based on CdSe/$Zn_{1-x}Cd_xS$ core/shell heterostructured quantum dots, Adv. Mater. 26 (2014) 8034–8040.
[18] W.Y. Ji, Y. Tian, Q.H. Zeng, S.N. Qu, L.G. Zhang, P.T. Jing, J. Wang, J.L. Zhao, Efficient quantum dot light-emitting diodes by controlling the carrier accumulation and exciton formation, ACS Appl. Mater. Interfaces 6 (2014) 14001–14007.
[19] B.Y. Ouyang, C.W. Chi, F.C. Chen, Q. Xu, Y. Yang, High-conductivity poly (3,4-ethylenedioxythiophene): poly(styrene sulfonate) film and its application in polymer optoelectronic devices, Adv. Funct. Mater. 15 (2005) 203–208.
[20] S. Jonsson, J. Birgersson, X. Crispin, G. Greczynski, W. Osikowicz, A.W.D. van der Gon, W.R. Salaneck, M. Fahlman, The effects of solvents on the morphology and sheet resistance in poly (3,4-ethylenedioxythiophene)-polystyrenesulfonic acid (PEDOT-PSS) films, Synth. Met. 139 (2003) 1–10.
[21] S. Timpanaro, M. Kemerink, F. Touwslager, M.M.D. Kok, S. Schrader, Morphology and conductivity of PEDOT/PSS films studied by scanning-tunneling microscopy, Chem. Phys. Lett. 394 (2004) 339–343.
[22] F. Louwet, L. Groenendaal, J. Dhaen, J. Manca, J. Van Luppen, E. Verdonck, L. Leenders, PEDOT/PSS: synthesis, characterization, properties and applications, Synth. Met. 135 (2003) 115–117.
[23] X. Crispin, S. Marciniak, W. Osikowicz, G. Zotti, A.W.D. van der Gon, F. Louwet, M. Fahlman, L. Groenendaal, F.D. Schryver, W.R.J. Salaneck, Conductivity, morphology, interfacial chemistry, and stability of poly(3,4-ethylene dioxythiophene)-poly(styrene sulfonate): a photoelectron spectroscopy study, Polym. Sci, Part B: Polym. Phys. 41 (2003) 2561–2583.
[24] T.J. Wang, Y.Q. Qi, J.K. Xu, X.J. Hu, P. Chen, Effects of poly(ethylene glycol) on electrical conductivity of poly (3,4-ethylenedioxythiophene)-poly (styrenesulfonic acid) film, Appl. Surf. Sci. 250 (2005) 188–194.

[25] J.Y. Kim, J.H. Jung, D.E. Lee, J. Joo, Enhancement of electrical conductivity of poly(3,4-ethylenedioxythiophene)/poly(4-styrenesulfonate) by a change of solvents, Synth. Met. 126 (2002) 311–316.
[26] Q. Wang, Y. Chen, Y. Zheng, N. Ai, S. Han, W. Xu, Z. Jiang, Y. Meng, D. Hu, J. Peng, J. Wang, Y. Cao, Solvent treatment as an efficient anode modification method to improve device performance of polymer light-emitting diodes, Org. Electron. 14 (2013) 548–553.
[27] H. Shen, Q. Lin, H. Wang, L. Qian, Y. Yang, A. Titov, J. Hyvonen, Y. Zheng, L.S. Li, Efficient and bright colloidal quantum dot light-emitting diodes via controlling the shell thickness of quantum dots, ACS Appl. Mater. Interfaces 5 (2013) 12011–12016.
[28] W.K. Bae, J.H. Kwak, J. Lim, D. Lee, M. Nam, K. Char, C.H. Lee, S. Lee, Deep blue light-emitting diodes based on $Cd_{1-x}Zn_xS$@ZnS quantum dots, Nanotechnology 20 (2009) 075202.
[29] L. Qian, Y. Zheng, K.R. Choudhury, D. Bera, F. So, J.G. Xue, P.H. Holloway, Electroluminescence from light-emitting polymer/ZnO nanoparticle heterojunctions at sub-bandgap voltages, Nano Today 5 (2010) 384–389.
[30] W.Y. Ji, P.T. Jing, J.L. Zhao, Improving the efficiency and reducing efficiency roll-off in quantum dot light emitting devices by utilizing plasmonic Au nanoparticles, J. Mater. Chem. C 1 (2013) 470–476.
[31] U. Lang, E. Mueller, N. Naujoks, J. Dual, Microscopical investigations of PEDOT: PSS thin films, Adv. Funct. Mater. 19 (2009) 1215–1220.